

Perturbation correction in the ionometric determination of absorbed dose
in a graphite phantom

by M. Boutillon

Institut National de la Santé et de la Recherche Médicale, Paris

1. Introduction

The determination of absorbed dose in graphite for ^{60}Co gamma rays is performed at the Bureau International des Poids et Mesures by means of a flat ionization chamber which is made of graphite and located in a graphite phantom.

For an ideal cavity which disturbs neither the photon nor the electron fluence, the absorbed dose D in graphite is given, according to the classical Bragg-Gray relation, by

$$D = \frac{1}{\bar{f}} \frac{dQ}{dm} \frac{W}{e} \quad (1)$$

where

\bar{f} is the mean ratio of the mass stopping powers of air and carbon,

dQ is the quantity of electricity liberated in the air mass dm ,

W is the average energy required to produce an ion pair in air and

e is the electronic charge.

However, in a practical situation the dimensions of the cavity are not negligible. The photon fluence and the electron fluence are disturbed. The energy liberated per mass unit of air in a real cavity will be different from that liberated in an ideal cavity. The ratio of these two quantities gives the perturbation correction k_p to be applied to the measured quantity to obtain the absorbed dose in the homogeneous graphite phantom at the center of the chamber in absence of the chamber.

The determination of the correction factor k_p is a difficult problem which we have tried to solve by using the same type of analysis as in [1, 2] for the determination of exposure at BIPM. In the present paper we confine ourselves to describing the main features of this correction. The other problems involved in the absorbed dose determination will be treated later in more detail.

2. Spectrum of the radiation

The spectrum of the scattered radiation inside the BIPM graphite phantom has been calculated for different depths by a Monte-Carlo method. Figure 1 shows the ratio $R = K_s/K_p$ of the kermas in graphite of the scattered and of the primary radiations as a function of depth in the phantom. The influence of a cavity on the scattered radiation has been investigated by means of a similar calculation. The cavity has a thickness $u = 2$ mm and is placed in the phantom at the reference depth corresponding to 5 g cm^{-2} .

In Fig. 2 the curves R_1 and R_2 are compared with $\rho'z$ (where ρ is the graphite density and z the distance from the source) in the vicinity of the reference position z_m , without and with cavity. It can be seen from the figure that for $z < z_m$ the two curves are practically the same and that for $z > z_m$ the presence of the cavity causes a shift of the curve which is very close to 2 mm. On the basis of these results we have assumed that for $z < z_m - u/2$ the kermas in graphite of the scattered radiation, $K_{s2}(z)$ with cavity, and $K_{s1}(z)$ without cavity, are the same and that, for $z > z_m + u/2$, $K_{s2}(z)$ is equal to $K_{s1}(z - u)$.

In addition, we can reasonably deduce from the shape of the curve R_1 that, for a small interval Δz which is sufficient to ensure electronic equilibrium, R_1 varies linearly with z . In the absence of a cavity this relation can be expressed by

$$R(z) = R(z_m) \left[1 - \beta (z_m - z) \right]. \quad (2)$$

3. Spatial distribution of the radiation

The phantom is cylindrical and the ^{60}Co source is placed on its axis, so that there is an axial symmetry of the whole system. Let us consider a slab of material dz (Fig. 3) which is traversed by photons giving birth to electrons in the slab. If the source is far enough, we can say that the photon fluence is uniform in this layer (at least in the region where the electrons produced have a chance to reach the cavity).

The angular distribution (with axial symmetry) of these photons was calculated by a Monte-Carlo method. Table 1 gives the results for the reference depth (5 g cm^{-2}). Although the figures are not precise, the error introduced in the result is negligible.

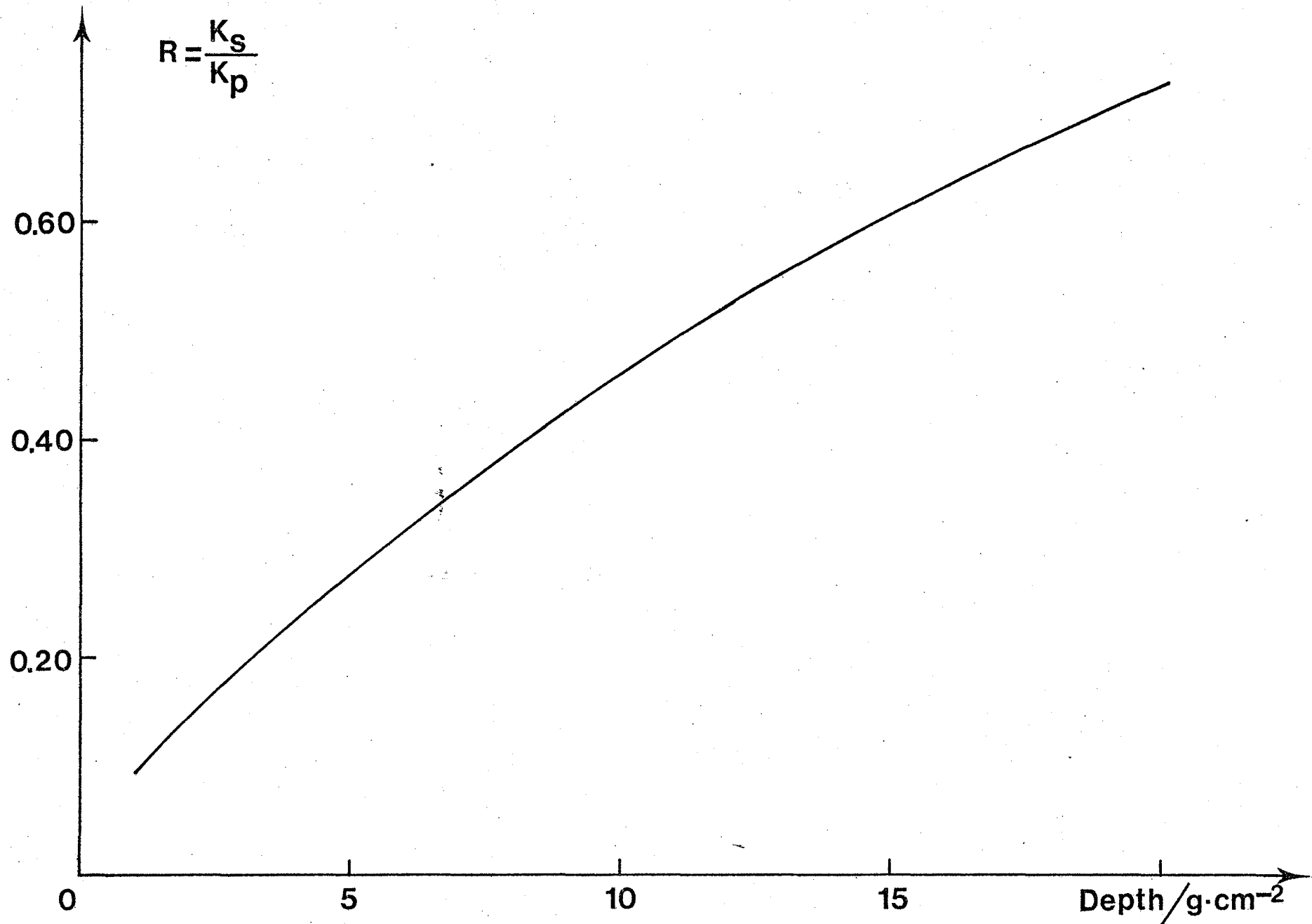


Figure 1 - Ratio R of kermas of scattered and unscattered photons in a homogeneous graphite phantom for the reference conditions of international absorbed dose comparisons.

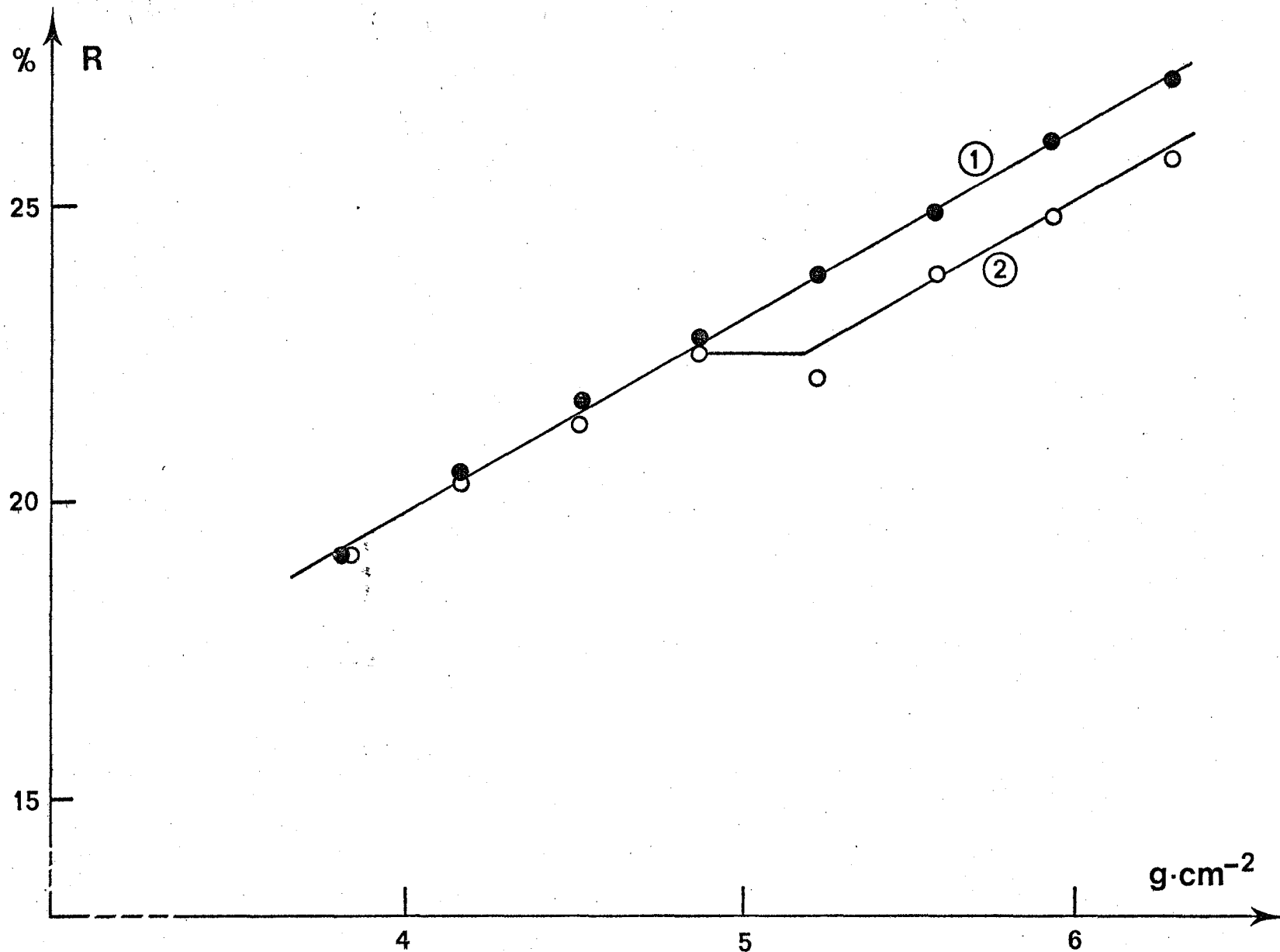


Figure 2 - Variation of R in the vicinity of the reference depth, with and without cavity.

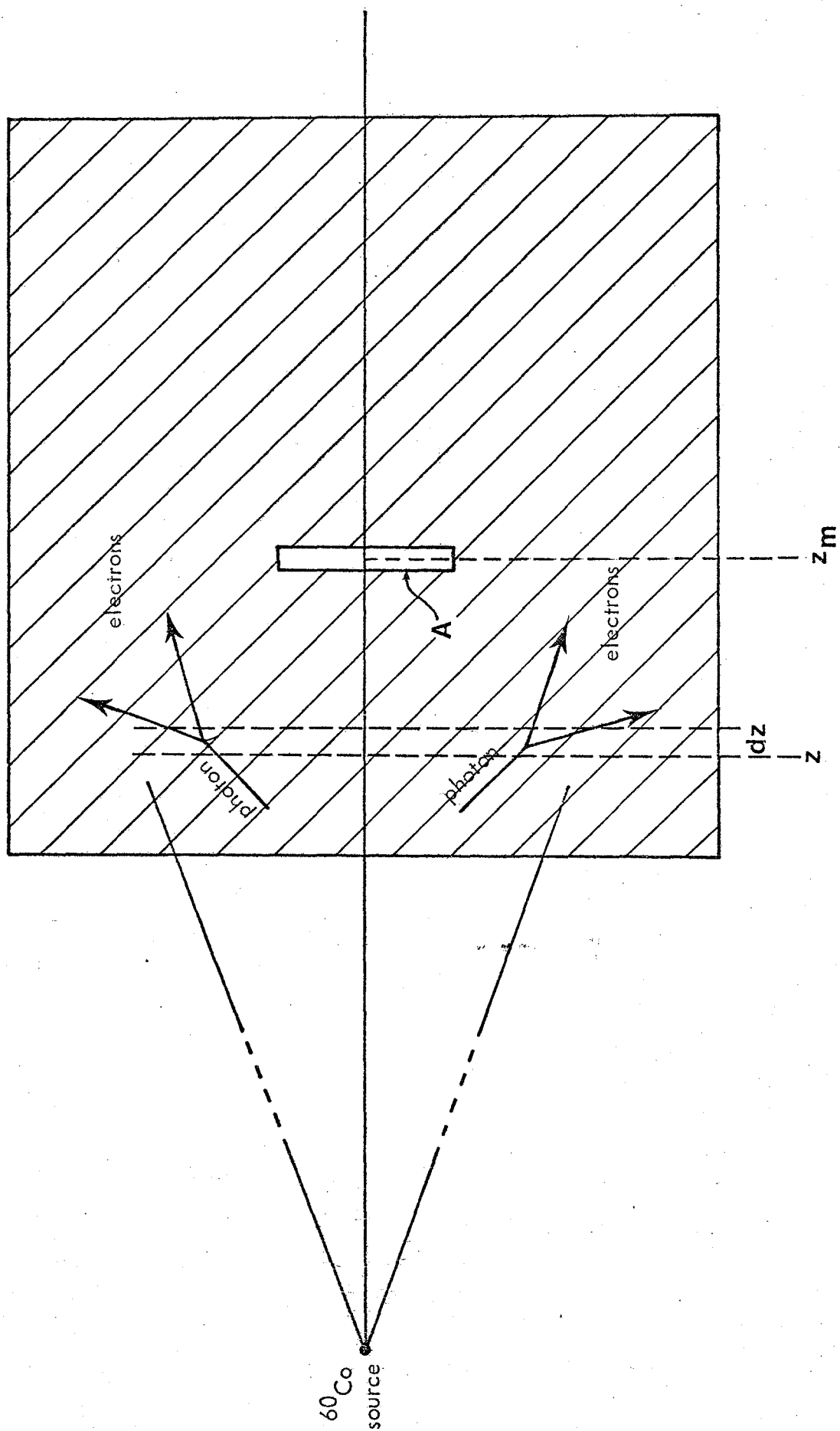


Figure 3 - Interaction of photons in the phantom.

Table 1

Angular photon distribution at the depth 5 g cm^{-2}

Percentage of photons for a given solid angle and energy interval						
angle energy (MeV)	0-30	30-60	60-90	90-120	120-150	150-180
0 - 0.1	0.06	0.16	0.12	0.17	0.33	0.16
0.1-0.2	0.07	0.20	0.12	0.16	0.30	0.15
0.2-0.3	0.02	0.05	0.05	0.18	0.44	0.26
0.3-0.4	0.06	0.12	0.31	0.42	0.08	0.01
0.4-0.5	0.03	0.12	0.82	0.03	0	0
0.5-0.6	0.03	0.51	0.46	0	0	0
0.6-0.7	0.025	0.91	0.065	0	0	0
0.7-0.8	0.01	0.98	0.01	0	0	0
0.8-0.9	0.03	0.97	0	0	0	0
0.9-1.0	0.62	0.38	0	0	0	0
1.0-1.1	0.996	0.004	0	0	0	0
1.1-1.2	1	0	0	0	0	0
1.2-1.25	1	0	0	0	0	0

4. Production and dissipation of the electrons

The slab of material dz traversed by the photons can be considered as a source of electrons which are produced by the photons in this slab. The electron fluence is uniform in the slab and its angular distribution can be deduced from the photon fluence by the Compton law. When photons of energy $h\nu$ produce an electron of energy T per unit area in the plane z , the moment method allows to calculate the energy released between two planes at the abscissae z_m and $z_m + dz_m$.

This energy is given by $\frac{T}{r'} (1 - G') g(T, h\nu, \frac{z_m - z}{r'}) dz_m$, where $g(T, h\nu, \frac{z_m - z}{r'})$ is the energy dissipation function and G' is the correction for bremsstrahlung.

The dissipation functions for the angular distribution determined above were calculated by the moment method [3].

5. Energy released in the cavity

The energy released in the cavity dz_m by electrons with energy between T and $T + dT$, which are produced in the slab dz by photons with energy between $h\nu$ and $h\nu + dh\nu$, is given by the relation

$$\frac{d^3 E}{dT dh\nu dz} = A \cdot \bar{\Phi}(h\nu, z) \cdot \frac{T}{r'} \frac{d\sigma'}{dT} \cdot (1 - G') \cdot g'(T, h\nu, x) dz_m \frac{\rho}{\rho'} \bar{F}, \quad (3)$$

where

A is the cavity section,

$\bar{\Phi}(h\nu, z)$ is the photon fluence,

$\frac{d\sigma'}{dT}$ is the Compton cross section

and $\frac{\rho}{\rho'} \bar{F}$ is the Bragg-Gray term.

The fluence term can be divided into two parts by writing

$$\bar{\Phi}(h\nu, z) = \bar{\Phi}_p(h\nu, z) + \bar{\Phi}_s(h\nu, z), \quad (4)$$

where the first term describes the primary radiation and the second the scattered radiation. If we integrate equation (3) over T and $h\nu$, we obtain

$$\frac{dE}{dz} = \left\{ \left[\bar{\Phi}_p(h\nu, z) \int_T \frac{1}{\rho'} T \frac{d\sigma'}{dT} \right] \frac{1}{r'} \bar{g}'(x) + \left[\int_{h\nu} \bar{\Phi}_s(h\nu, z) \int_T \frac{1}{\rho'} T \frac{d\sigma'}{dT} \right] \frac{1}{r'} \bar{g}'(x) \right\} \cdot \bar{F} \cdot (1 - \bar{G}') A \rho dz_m,$$

where the terms with bars are the mean values averaged over the corresponding spectra.

Since the two expressions within the brackets are equal to the kerma $K_p(z)$ in graphite of the primary photons and to the kerma $K_s(z)$ in graphite of the scattered photons, respectively, equation (5) may be written as

$$\frac{dE}{dz} = A \rho dz_m \bar{f} (1 - \bar{G}') \left\{ K_p(z) \cdot \frac{1}{r'} \bar{g}'(x) + K_s(z) \frac{1}{r'} \bar{\bar{g}}'(x) \right\}. \quad (6)$$

We have then to integrate equation (6) over z (z varies between $(-\infty, +\infty)$ for a very thin cavity and between $(-\infty, -u)$ and $(u, +\infty)$ for a cavity of thickness $2u$).

6. Determination of the perturbation correction k_p

$K_p(z)$ is related to the kerma in graphite $K_p(z_m)$ in the plane z_m for a very thin cavity by the relation

$$K_p(z) = K_p(z_m) \cdot \exp \left[\mu'(z_m - z) \right] \cdot z^2 / z_m^2,$$

where μ' is the linear attenuation coefficient of the primary beam in graphite and $K_s(z)$ is related to $K_p(z)$ by the relations given in section 2.

We omit the details of the calculation which is tedious and restrict ourselves to indicating the results. For a very thin cavity we obtain

$$\frac{E_o}{m_o} = K_p(z_m) \cdot \bar{f} \cdot (1 - \bar{G}') \underbrace{\left\{ \left[1 + \left(\mu' + \frac{2}{z_m} \right) r' \bar{x}' \right] + R(z_m) \left[1 + \left(\mu' + \frac{2}{z_m} - \beta \right) r' \bar{\bar{x}}' \right] \right\}}_{B_o}, \quad (7)$$

where m_o is the mass of the gas, and \bar{x}' and $\bar{\bar{x}}'$ are the first moments of the mean dissipation function $\bar{g}'(x)$ and $\bar{\bar{g}}'(x)$ for electrons produced by primary and scattered photons, respectively.

For a cavity of thickness $2u$, with a collecting electrode of thickness v located in the middle, we obtain

$$\frac{E}{m} = K_p(z_m) \bar{f} \cdot (1 - \bar{G}') \cdot e^{\mu' u} \cdot \underbrace{\left\{ \left[1 + \left(\mu' + \frac{2}{z_m} \right) r' \bar{x}' + \frac{u}{z_m} (F(o) + F(v/r')) \right] + R(z_m) \left[1 + \left(\mu' + \frac{2}{z_m} - \beta \right) r' \bar{\bar{x}}' - \beta u + \frac{2u}{z_m} \right] \right\}}_B, \quad (8)$$

$$\text{where } F(x) = \int_x^1 \bar{g}(x) dx - \int_{-1}^{-x} \bar{g}(x) dx.$$

The correction factor k_p to be applied is

$$k_p = \frac{E_o/m_o}{E/m} = e^{-\mu'u} \frac{B_o}{B} . \quad (9)$$

Table 2 gives the values of the parameters entering in the determination of k_p and their uncertainties for the reference depth 5 g cm^{-2} . The calculation was made taking into account the successive slabs of material in front and behind the cavity. However, in the case of a thick cavity, a part λ of the energy lost is due to the electrons produced in the lateral wall. For these electrons we assume that no correction has to be made. Then the total correction to be applied is

$$k'_p = \frac{E_o/m_o}{\lambda E_o/m_o + (1-\lambda) E/m} = \frac{B_o}{\lambda B_o + (1-\lambda) e^{\mu'u} B} . \quad (10)$$

The value of λ for the BIPM ionization chamber is assumed to be 0.165; the corresponding uncertainty in k'_p is about 0.1 %. The variation of k'_p with depth is given in Figure 4.

The BIPM ionization chamber was compared with calorimeters of other national laboratories (NBS, LMRI, PTB and RIV) using the values of k'_p determined above. The good agreement suggest that k'_p is fairly well determined, justifying thereby the approximations made in the calculation.

Table 2

Values of the parameters entering in the determination of k_p for the reference depth 5 g cm^{-2}

$z_m = 1 \text{ m} \quad u = 2 \text{ mm} \quad v = 1 \text{ mm}$

$$k_p = e^{-\mu' u} \frac{1 + (\mu' + \frac{2}{z_m}) \bar{r} \bar{x}' + R(z_m) \left[1 + (\mu' + \frac{2}{z_m} - \beta) \bar{r} \bar{x}' \right]}{1 + (\mu' + \frac{2}{z_m}) \bar{r} \bar{x}' + \frac{u}{z_m} \left[F(0) + F\left(\frac{v}{r}\right) \right] + R(z_m) \left[1 + (\mu' + \frac{2}{z_m} - \beta) \bar{r} \bar{x}' - \beta u + \frac{2u}{z_m} \right]}$$

values	0.978 3	0.80 %	0.24 %	0.27	- 0.36 %	5.37 %
uncertainty of these values	0.03 %	0.1 %	0.05 %	0.5 %	0.2 %	0.5 %
resulting uncertainty of k_p	0.03 %	$< 10^{-5}$	0.04 %	0.02 %	$< 10^{-5}$	0.11 %

Total uncertainty of k_p (quadratic sum) = 0.12 %

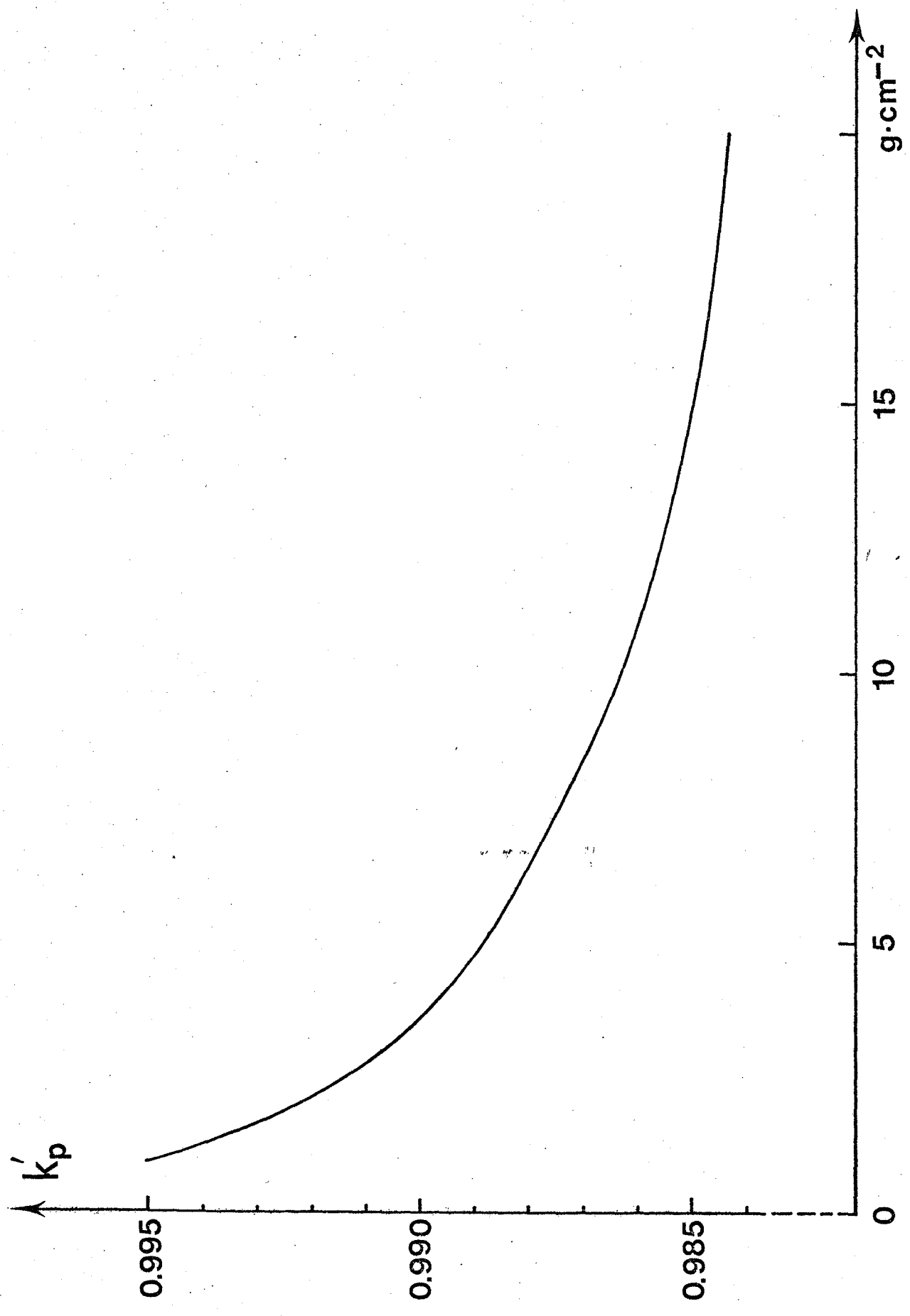


Figure 4 - Correction k'_p applied to the BIPM chamber.

- [1] A. Allisy, Contribution à la mesure de l'exposition produite par les photons émis par le ^{60}Co , *Metrologia* 3, 2, 1967, p. 41, and *Recueil de Travaux du Bureau International des Poids et Mesures* 1, 1966-1967
- [2] M. Boutillon and M.-T. Niatel, A study of a graphite cavity chamber for absolute exposure measurements of ^{60}Co gamma rays, *Metrologia* 9, 4, 1973, p. 139, and *Recueil de Travaux du Bureau International des Poids et Mesures* 4, 1973-1974
- [3] L.V. Spencer, Energy dissipation by fast electrons, NBS Monograph 1, 1959.

(July 1979)
